ANTIOXIDANTS & REDOX SIGNALING
Volume 21, Number 11, 2014

DOI: 10.1089/ars.2013.5404

Therapeutics

FORUM ORIGINAL RESEARCH COMMUNICATION

Increased Antioxidant Defense Mechanism in Human Adventitia-Derived Progenitor Cells Is Associated with Therapeutic Benefit in Ischemia

Dominga Iacobazzi,[1,2] Giuseppe Mangialardi,[1] Miriam Gubernator,[1] Manuela Hofner,[3] Matthias Wielscher,[3] Klemens Vierlinger,[3] Carlotta Reni,[1] Atsuhiko Oikawa,[1] Gaia Spinetti,[4] Rosa Vono,[4] Elena Sangalli,[4] Monica Montagnani,[2] and Paolo Madeddu[1]

Abstract

Aims: Vascular wall-resident progenitor cells hold great promise for cardiovascular regenerative therapy. This study evaluates the impact of oxidative stress on the viability and functionality of adventitia-derived progenitor cells (APCs) from vein remnants of coronary artery bypass graft (CABG) surgery. We also investigated the antioxidant enzymes implicated in the resistance of APCs to oxidative stress-induced damage and the effect of interfering with one of them, the extracellular superoxide dismutase (EC-SOD/SOD3), on APC therapeutic action in a model of peripheral ischemia. ***Results:*** After exposure to hydrogen peroxide, APCs undergo apoptosis to a smaller extent than endothelial cells (ECs). This was attributed to up-regulation of antioxidant enzymes, especially SODs and catalase. Pharmacological inhibition of SODs increases reactive oxygen species (ROS) levels in APCs and impairs their survival. Likewise, APC differentiation results in SOD down-regulation and ROS-induced apoptosis. Oxidative stress increases APC migratory activity, while being inhibitory for ECs. In addition, oxidative stress does not impair APC capacity to promote angiogenesis *in vitro*. In a mouse limb ischemia model, an injection of naïve APCs, but not SOD3-silenced APCs, helps perfusion recovery and neovascularization, thus underlining the importance of this soluble isoform in protection from ischemia. ***Innovation:*** This study newly demonstrates that APCs are endowed with enhanced detoxifier and antioxidant systems and that SOD3 plays an important role in their therapeutic activity in ischemia. ***Conclusions:*** APCs from vein remnants of CABG patients express antioxidant defense mechanisms, which enable them to resist stress. These properties highlight the potential of APCs in cardiovascular regenerative medicine. *Antioxid. Redox Signal*. 21, 1591–1604.

Introduction

REACTIVE OXYGEN SPECIES (ROS) play important roles in the regulation of cell homeostasis. ROS include radical species such as superoxide (O_2^{-}) and hydroxyl radical ($HO^{\bullet}$) as well as nonradical species such as hydrogen peroxide (H_2O_2). Under physiologic conditions, moderate levels of ROS act as a second messenger in various signaling pathways, ensuring that cells respond properly to specific stimuli. On the other hand, excessive increase in ROS production or reduction of antioxidant defense mechanisms can disrupt the redox balance and induce DNA damage and cell death (24, 28, 33, 36, 37).

Appropriate redox homeostasis is also important for the maintenance of stem cell (SC) self-renewal (12, 27). In SCs, intracellular ROS levels are regulated by a very efficient system of antioxidant enzymes, including catalase and superoxide dismutases (SODs) (27). Moreover, the low-oxygenic niche provides SCs with extra-protection from oxidative stress (17). The disruption of endogenous and

[1]Expermental Cardiovascular Medicine, School of Clinical Sciences, University of Bristol, Bristol, United Kingdom.
[2]Department of Biomedical Sciences and Human Oncology, University of Bari, Medical School, Bari, Italy.
[3]AIT-Austrian Institute of Technology, Vienna, Austria.
[4]Laboratory of Diabetological Research IRCCS MultiMedica, Milan, Italy.

Innovation

Owing to their rarity, adventitia-derived progenitor cells (APCs) need to be expanded *ex vivo* in order to obtain sufficient numbers for clinical use. Culture expansion might lead to cell senescence and functional incompetence. Our data show for the first time that repeatedly passaged APCs from cardiovascular patients maintain an intact antigenic phenotype and high defense mechanisms. This culminates in reduced apoptosis, high proliferation and migratory activity, as well as preserved pro-angiogenic potential after exposure to reactive oxygen species or transplantation into ischemic muscles, thus highlighting that APCs have a potential in cardiovascular regenerative medicine.

environmental defence mechanisms due to aging and disease can trigger SC differentiation and damage, with a profound impact on associated regenerative mechanisms (33, 38). With regard to vascular precursors, these phenomena have been initially investigated in endothelial progenitor cells (EPCs), a heterogeneous population of mononuclear cells that are able to promote vascular repair (10). It remains unknown whether the same concepts apply to pericytes, which, besides constituting a physical and functional interface between endothelial cells (ECs) and the extravascular space, are thought to represent a resident population of vascular progenitors (4, 30).

To date, two distinct pericyte populations have been identified on the basis of localization and antigenic characteristics. The first subtype resides around the microvasculature of various organs and expresses a spectrum of antigens, such as CD146, PDGFRβ, and NG2, which are also shared by endothelial, smooth muscle, and glial cells. The second subtype is contained in the blood vessel wall in close vicinity to the adventitial *vasa vasorum* (5, 7, 16, 23, 35). Adventitia-derived progenitor cells (APCs) have several markers in common with microvascular pericytes, except for CD146, and also carry mesenchyme-specific antigens, such as CD44, CD90, CD73, and CD29, as well as SC markers, such as Oct-4, GATA-4, and Sox-2 (5). The latter characteristics, coupled with recognition of clonogenicity and multipotency, have led to a consideration of APCs as precursors of definitive pericytes. Furthermore, APCs are in the focus of intense translational research because of their potent reparative potential. Our group was the first to demonstrate that APCs, isolated from saphenous veins of patients undergoing coronary artery bypass graft (CABG) surgery, promote reparative neovascularization and accelerate tissue healing, when injected in models of myocardial and peripheral ischemia (5, 16, 18). Transplanted APCs are able to home to neovessels, establishing close anatomic connections and paracrine interactions with resident ECs. Therefore, APCs appear particularly adaptable to the harsh environment of an ischemic tissue. Nonetheless, mechanisms underlying this adaptability remain unknown.

The aim of the present study was to investigate: (i) the impact of oxidative stress on different functional activities of APCs, with cross-reference to cells derived from APC differentiation, microvascular pericytes, fetal ECs, and saphenous vein-derived ECs (SVECs); (ii) the molecular mechanisms underlying APC resistance to oxidative stress; and (iii) the consequences of silencing the soluble SOD isoform (SOD3) on APC therapeutic activity in a murine model of limb ischemia.

Results

Characterization of APC and SVEC antigenic profile

First, by immunocytochemistry and flow cytometry, we confirmed that cultured human APCs coexpress typical pericyte/mesenchymal antigens (Fig. 1A, B). In addition, APCs were positive for CD105, which is predominantly expressed on cellular lineages within the vascular system, and negative for hematopoietic (CD45) and endothelial (CD31) markers. This phenotype was consistently confirmed from early to late passages (from P3 to P7, data not shown). In contrast, SVECs were identified positive for VE-cadherin and CD31 by immunocytochemistry (Fig. 1C) and for CD44, CD105, and CD31 by flow cytometry (Fig. 1D).

APCs exhibit a higher resistance to oxidative stress as compared with ECs

Next, we determined the levels of intracellular ROS in APCs, human umbilical vein ECs (HUVECs), and SVECs under basal conditions and after stimulation with increasing doses of H_2O_2. To this aim, a live cell imaging approach was used on cells loaded with the Mitotracker CM-H_2XRos probe. Confocal imaging analysis showed that exposure to H_2O_2 induces a dose-dependent increase in ROS concentration in HUVECs and SVECs, whereas this effect was not observed in APCs (Fig. 2A, B). Two-way ANOVA showed an effect of the H_2O_2 dose ($p = 0.01$) and cell type ($p = 0.008$) on ROS levels. The antioxidant N-Acetyl Cysteine contrasted the effect of H_2O_2 in HUVECs and SVECs (Fig. 2C–E).

Next, we analyzed the susceptibility of APCs and ECs to oxidative stress-induced apoptosis. As shown in Figure 2F, H_2O_2 increased Caspase 3/7 activity in both HUVECs and SVECs, but not in APCs. Two-way ANOVA confirmed an effect of the H_2O_2 dose ($p < 0.0001$) and cell type ($p = 0.01$) on apoptosis.

Furthermore, we analyzed protein carbonyl levels in HUVECs and APCs as a biomarker of oxidative stress (8). As illustrated in Supplementary Figure S1A (Supplementary Data are available online at www.liebertpub.com/ars), HUVECs showed increased protein carbonylation after exposure to H_2O_2, while this phenomenon was not observed in APCs. Two-way ANOVA confirmed an effect of cell type on carbonylation ($p < 0.01$). Similarly, staining of phosphorylated form of γH2AX, a biomarker of double-strand DNA breaks (9), is increased in HUVECs after exposure to different concentrations of H_2O_2, a phenomenon that was observed in APCs only when elevating oxidative stress to very high levels (250 m*M* H_2O_2) (Supplementary Fig. S1B, C). These data support the concept that APCs have a greater resilience under oxidative stress.

APCs exhibit increased antioxidant activity

Having demonstrated that APCs are less susceptible to ROS-induced damage than ECs, we next asked whether this resistance is attributable to constitutive expression of antioxidant mechanisms. Results from gene array experiments indicate that among the 1375 genes that are differently expressed between APCs and HUVECs with a log FC > 1.5

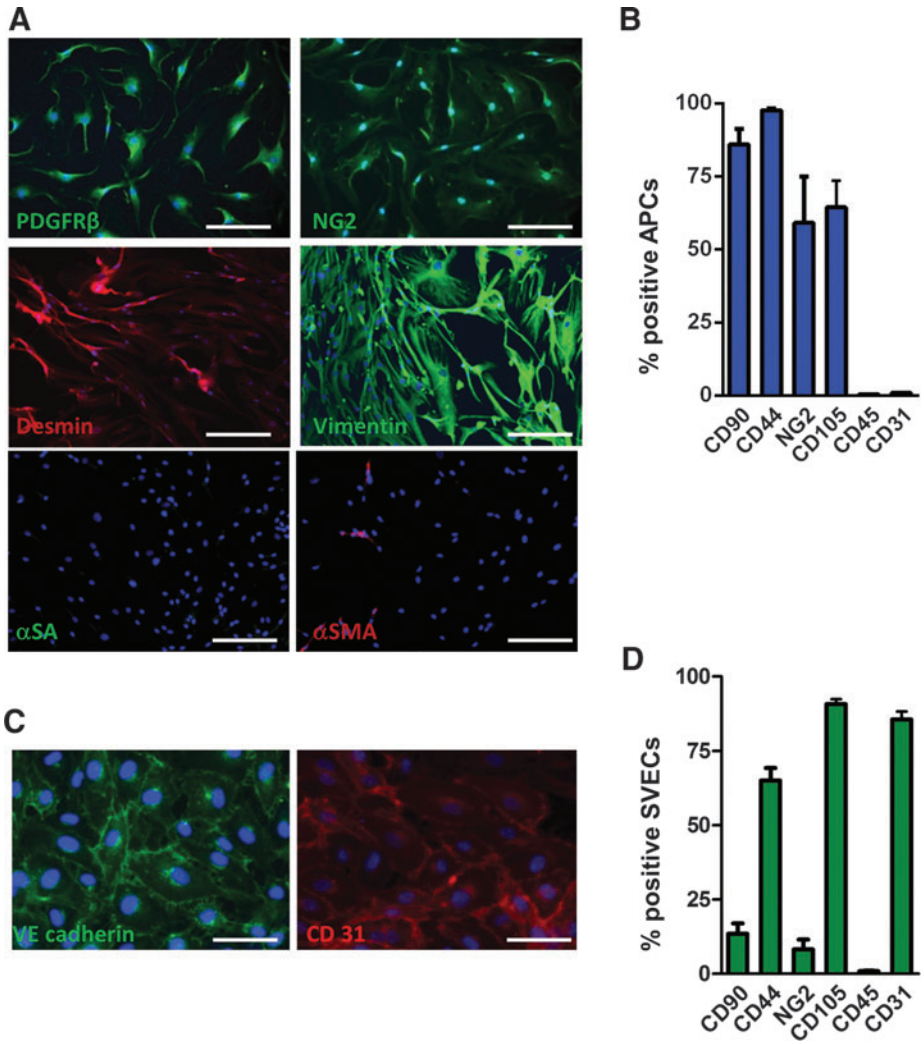

FIG. 1. Antigenic profile of human adventitia-derived progenitor cells (APCs) and saphenous vein-derived endothelial cells (SVECs). (A) Representative microscopy images showing the antigenic profile of APCs at passage 7: Cells express typical pericyte/mesenchymal markers, such as PDGFRβ, NG2, desmin, and vimentin, while showing scarce abundance or absence of α-sarcomeric actin (α-SA) or α-smooth muscle actin (α-SMA). Scale bar = 200 μm. **(B)** Flow cytometry characterization of APC immunogenic profile: bar graph illustrating the average of six biological replicates. **(C, D)** SVECs express endothelial markers, such as VE-cadherin and CD31 as assessed by immunocytochemistry **(C)** and flow cytometry **(D)**. Endoglin (CD105) and CD44 are expressed in both APCs and SVECs. Data are mean ± SEM. To see this illustration in color, the reader is referred to the web version of this article at www.liebertpub.com/ars

and $p < 0.001$, 20 genes involved in oxidation-reduction processes are up-regulated in APCs (Table 1). Notably, APCs express four-fold higher levels of aldehyde dehydrogenase, which exerts multiple biological activities, including drug resistance, cell differentiation, and oxidative stress response (11, 25). SODs are enzymes that catalyze the conversion of superoxide and inhibit the oxidative inactivation of nitric oxide, thereby preventing peroxynitrite formation and mitochondrial dysfunction (13). Owing to their different subcellular and extra-cellular localization, different SOD isoforms are thought to exert distinct functions. We found that levels of extra-cellular SOD3 are 6.3-fold higher in APCs compared with HUVECs (Fig. 3A). In contrast, APCs express remarkably lower levels of nicotinamide adenine dinucleotide phosphate-oxidase-4 (Nox4), an enzyme that has constitutive ROS-producing activity (Table 1) (2).

Quantitative real-time PCR confirmed that APCs express higher levels of SODs, especially of the SOD3 isoform, and of catalase, which converts hydrogen peroxide to water and oxygen, as compared with HUVECs or SVECs (Fig. 3B). Furthermore, we found that APCs abundantly express SOD1 and SOD2 proteins (Fig. 3C, D). Likewise, APCs secrete SOD3 in the conditioned culture medium (CCM) in larger amounts as compared with ECs (Fig. 3E, F). In order to determine whether SOD3 confers protection from oxidative stress, we next knocked down the expression of this enzyme by silencing its gene (Supplementary Fig. S2). The level of ROS detected in the SOD3-silenced APCs was only slightly increased in comparison to the negative control, either in basal conditions or after the H_2O_2 challenge (Fig. 4A, B). Likewise, no significant difference was detected between control and SOD3-silenced cells with regard to H_2O_2-induced apoptosis (data not shown). This might be due to the offsetting activity of the other antioxidant enzymes, including SOD1 and SOD2, which still take part in the ROS detoxification. Therefore, we next antagonized the global activity of SODs in APCs using the generic inhibitor diethyldithiocarbamate (DDC) (6, 32). SOD inhibition resulted in an increase of oxidative stress (Fig. 4C, D) and H_2O_2-induced apoptosis (Fig. 4E), thus confirming the prominent and synergistic role of SODs in APC protection from oxidative stress.

Down-regulation of antioxidant mechanisms after APC differentiation

Enhanced antioxidant and detoxifying activity has been associated to stemness (10). We previously reported that APCs express SC makers, such as Oct-4, GATA-4, and Sox-2, and possess clonogenic and multilineage differentiation

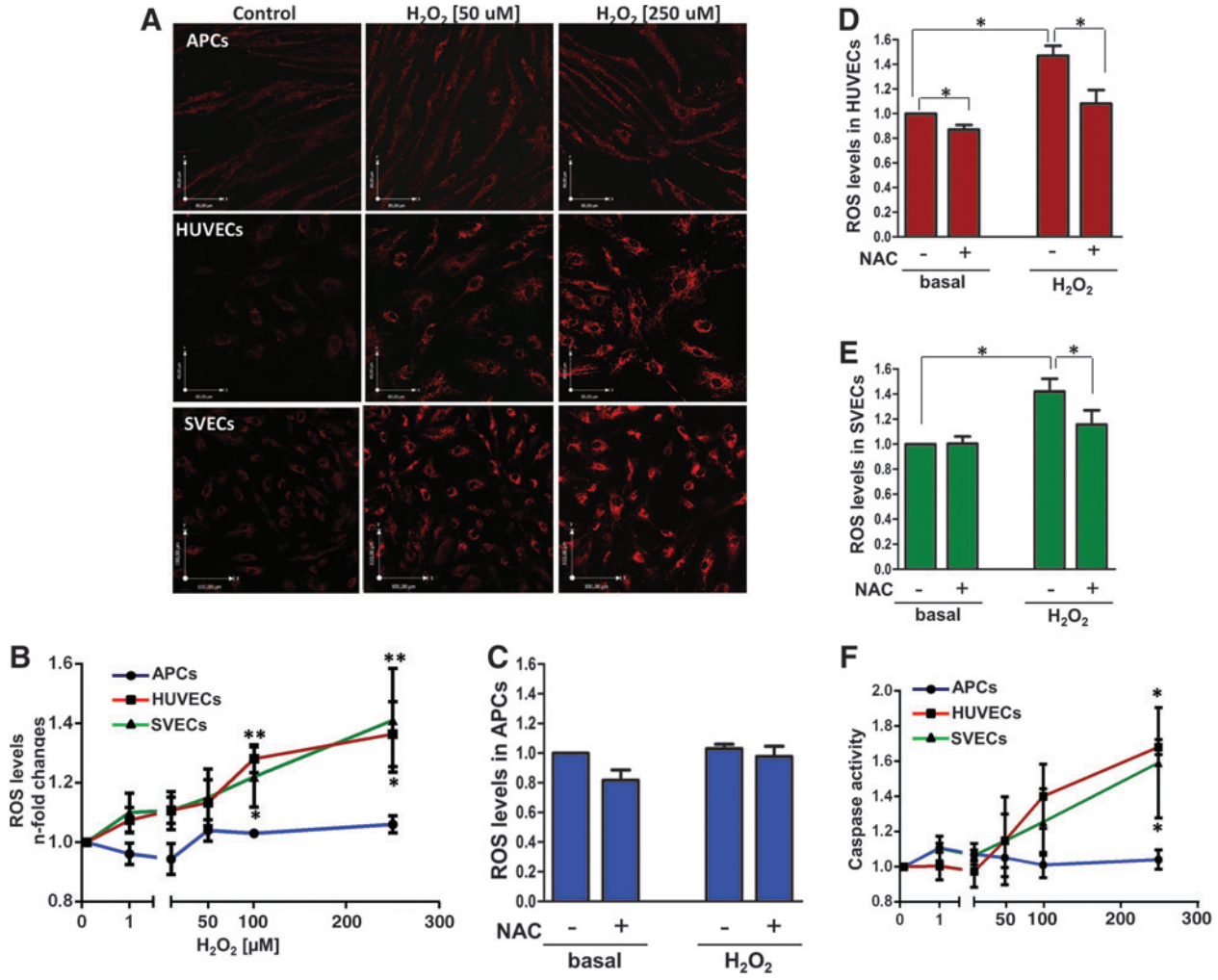

FIG. 2. APCs are resistant to oxidative stress. (A) Typical confocal microscopy images of reactive oxygen species (ROS), detected using the Mitotracker red tracer in APCs, human umbilical vein endothelial cells (HUVECs), and SVECs, under basal conditions (control) and after exposure to increasing doses of H_2O_2. **(B)** Line graph showing the average values of ROS in APCs, HUVECs, and SVECs ($n = 3$ biological replicates per group, each assayed in triplicate). HUVECs and SVECs, but not APCs, exhibit a dose-dependent increase in ROS levels. Values represent fold change *versus* vehicle and are expressed as means ± SEM. $*p < 0.05$; $**p < 0.01$ *versus* control in each group. **(C–E)** *In situ* detection of ROS in APCs, HUVECs, and SVECs, exposed to H_2O_2 (250 μM, 24 h) in the absence or presence of N-Acetyl Cysteine (NAC). NAC (1 mM, added 30 min before H_2O_2) prevents H_2O_2–induced oxidative stress in HUVECs and SVECs. Quantitative analysis of red fluorescence: Each bar is the mean ± SEM of three independent experiments, $*p < 0.05$ as indicated by the connecting line. **(F)** Effect of H_2O_2 on cell apoptosis: APCs, HUVECs, and SVECs were incubated with the indicated doses of H_2O_2 for 24 h. Apoptosis, as detected by Caspase 3/7 activity assay, was dose dependently increased in HUVECs and SVECs, but not in APCs. Each point is the mean ± SEM of three independent experiments, $*p < 0.05$ *versus* control in each group. To see this illustration in color, the reader is referred to the web version of this article at www.liebertpub.com/ars

capacities (5). Interestingly, here we report new results showing that induction of differentiation results in ~40% of APCs becoming adipocytes (Fig. 5A) with concomitant reduction in the expression of catalase, at mRNA level, and SODs, at both mRNA and protein levels (Fig. 5B–D). Furthermore, differentiated cells showed a remarkably increased susceptibility to apoptosis on exposure to H_2O_2 compared with native APCs (Fig. 5E). In addition, we compared the expression of antioxidant enzymes in APCs and microvascular pericytes extracted from limb skeletal muscles. Quantitative RT-PCR shows that, in comparison with microvascular pericytes, APCs exhibit higher levels of SOD1 and SOD2, while no difference was found in catalase and SOD3 expression. Furthermore, no significant difference between the two populations was detected when oxidative stress-induced apoptosis was evaluated (Supplementary Fig. S3A, B).

Additional functional consequences of oxidative stress in ECs and APCs

In addition to cell viability, ROS can affect a spectrum of cellular functions. Therefore, we performed a series of functional assays to investigate whether APCs and terminally differentiated vascular cells are programmed to respond to increased ROS levels in different ways. Exposure to high doses of H_2O_2 (100–250 μM) produced similar reductions in APC and EC proliferation, as assessed by the BrdU

Table 1. Antioxidant Genes Differently Expressed in APCs and HUVECs

Gene name	*LogFC*	*AveExpr*	*T*	*Adj.P.Val*
Superoxide dismutase 3, extracellular	6.28	7.87	10.28	2.71E-04
NADPH oxidase4	−6.13	8.37	−8.48	6.89E-04
Aldo-keto reductase family 1, member C1	5.20	8.69	17.53	2.06E-05
Dehydrogenase/reductase family 1, member B10 (aldose reductase)	4.44	8.28	7.30	1.38E-03
Aldehyde dehydrogenase 1 family, member L2	4.07	8.35	13.08	8.51 E-05
Cytochrome b reductase 1	3.70	11.70	13.13	8.42E-05
Thioredoxin interacting protein	3.20	12.08	9.83	3.39E-04
Sulfide quinone reductase-like	3.04	13.65	11.29	1.68E-04
Glutathione peroxidase 3	1.46	6.56	4.67	0.01007
Superoxide dismutase 2, mitochondrial	2.66	12.33	12.69	9.53E-05
Thioredoxin domain containing 15	2.33	8.18	12.16	1.15E-04
Xanthine dehydrogenase	2.28	5.82	6.57	0.00221
Thioredoxin domain containing 17	2.27	8.68	13.44	7.53E-05
Aldo-keto reductase family1, member B10 (aldose reductase)	2.23	6.58	7.76	0.00107
Glutathione peroxidase 7	1.86	8.20	4.26	0.01454
Carbonyl reductase 1	1.80	11.92	6.79	0.00191
Cytocrome b5 reductase 2	1.79	11.01	4.82	0.00883
Aldo-keto reductase family1, member C3	1.79	11.82	6.98	0.00168
Cytocrome b5 reductase 3	1.63	9.96	6.29	0.00272
Aldose reductase	1.62	5.98	5.03	0.00728
Glutathione peroxidase 3	1.46	6.56	4.67	0.01000

APC, adventitia-derived progenitor cell; HUVEC, human umbilical vein endothelial cell.

incorporation assay. However, in APCs only, low concentrations of H_2O_2 (1–10 μM) caused an increase in proliferation (Supplementary Fig. S4).

The migratory activity of cells exposed to H_2O_2 was evaluated using a scratch assay. As a stimulus, we used vascular endothelial growth factor (VEGF) for HUVECs and SVECs, and platelet-derived growth factor (PDGF) for APCs, as VEGF was a less strong stimulus for APCs (Supplementary Fig. S5A). This is likely due to the lack of VEGFR2 expression in pericytes as well as in mesenchymal

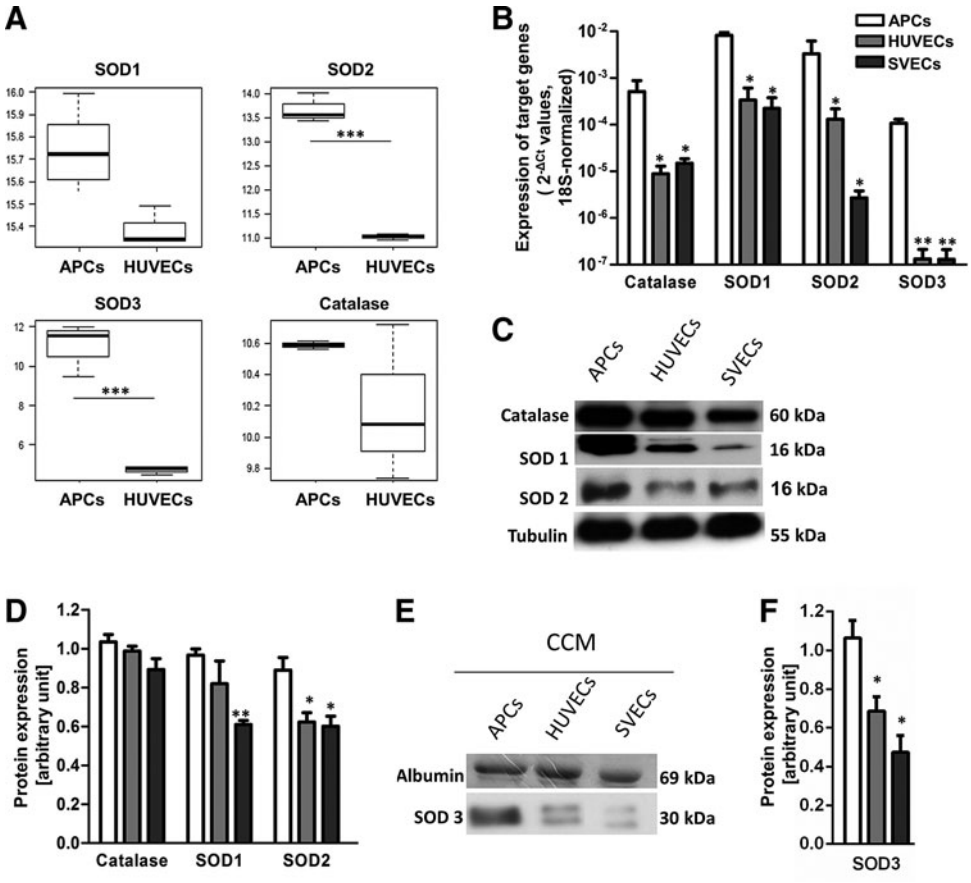

FIG. 3. APCs express higher levels of antioxidant enzymes as compared with endothelial cells (ECs). (A) Differential expression of antioxidant enzymes in HUVECs and APCs, as assessed by gene array: Data are expressed as median and max-min values, ***$p < 1e^{-}05$. **(B)** Catalase and SODs mRNA levels in APCs, HUVECs, and SVECs, as assessed by quantitative PCR: Data are means ± SEM of $n = 3$ biological replicates, *$p < 0.05$; **$p < 0.01$ *versus* APCs. **(C)**, Representative Western blot of Catalase and SODs. **(D)** Densitometry analysis and blot quantification: Data are means ± SEM of $n = 3$, *$p < 0.05$ *versus* APCs. **(E)** Western blot showing SOD3 expression in APC and EC conditioned culture media (CCM). **(F)** Bar graph showing the quantification of SOD3 protein levels in CCM by densitometric analysis: Data are means ± SEM of $n = 3$, *$p < 0.05$ *versus* APCs.

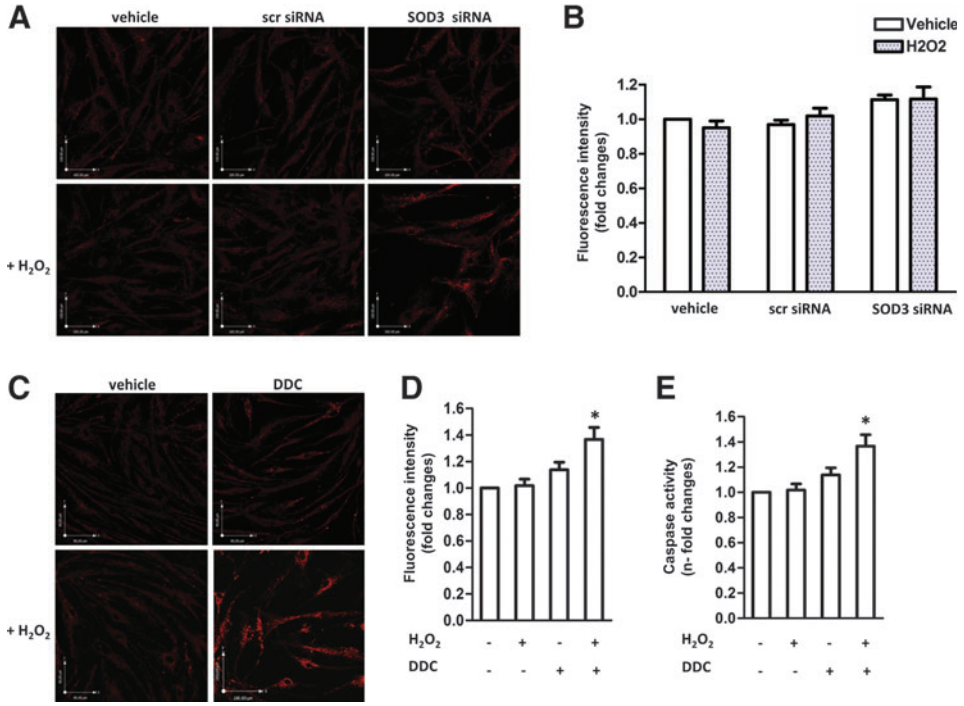

FIG. 4. Effects of SOD3 gene silencing and global SOD inhibition on H_2O_2- induced oxidative stress and apoptosis in APCs. (A) Fluorescent *in situ* detection of ROS in controls (APCs exposed to the transfection vehicle or transfected with scrambled (scr siRNA sequence) and SOD3-silenced APCs after exposure to H_2O_2 (250 μM, 24 h). **(B)** Histograms of oxidative stress levels under basal conditions and after exposure of APCs to H_2O_2 in the three groups described earlier: Data are means ± SEM of $n = 3$ replicates. **(C)** Fluorescent *in situ* detection of ROS in APCs exposed to H_2O_2 (250 μM, 24 h) in the absence or presence of diethyldithiocarbamate (DDC) (10 μM, 30 min before H_2O_2 addition). SOD inhibition with DDC enhances ROS levels under oxidant conditions. **(D)** Histograms illustrating the effect of H_2O_2 and/or DDC: Data are means ± SEM of $n = 3$, $^*p < 0.05$ *versus* respective control (no DDC). **(E)** Apoptosis, detected by the Caspase 3/7 activity assay, was also increased after global SOD inhibition. Data are means ± SEM of $n = 3$, $^*p < 0.05$ *versus* control. To see this illustration in color, the reader is referred to the web version of this article at www.liebertpub.com/ars

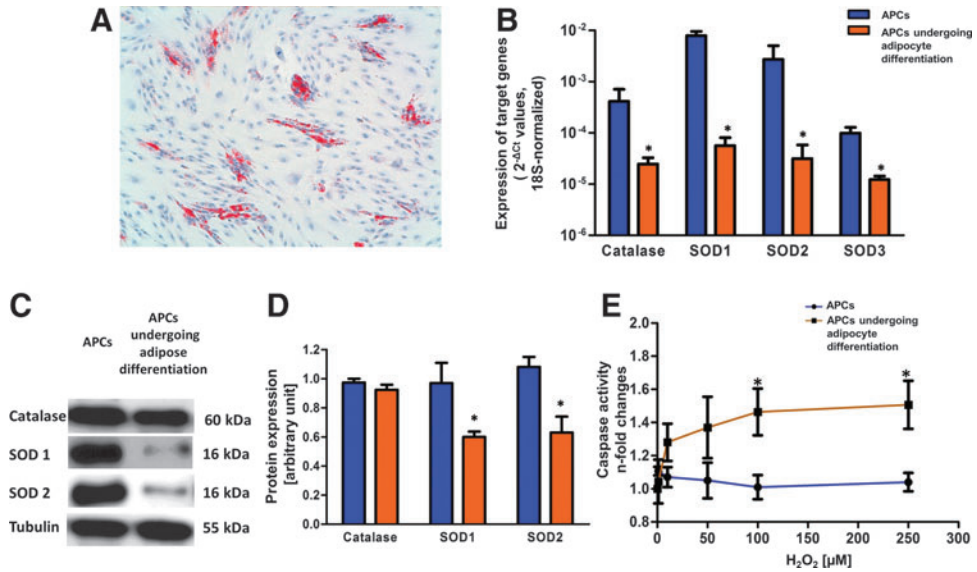

FIG. 5. The antioxidant activity of APCs is reduced after differentiation into adipocytes. (A) Red Oil O staining showing APCs undergoing adipocyte differentiation. **(B)** Catalase and SODs mRNA levels in APCs and APC-derived adipocytes, as assessed by quantitative PCR: Data are means ± SEM of $n = 3$ biological replicates, $^*p < 0.05$ *versus* APCs. **(C)** Representative Western blot of Catalase and SODs. **(D)** Densitometry analysis and blot quantification: Data are means ± SEM of $n = 3$, $^*p < 0.05$ *versus* APCs. **(E)** Effect of H_2O_2 on apoptosis: APCs and APC-derived adipocytes were incubated with the indicated doses of H_2O_2 for 24 h. Apoptosis, as detected by Caspase 3/7 activity assay, was dose dependently increased in APC-derived adipocytes, but not in APCs. Each point is the mean ± SEM of three independent experiments, $^*p < 0.05$ *versus* control in each group. To see this illustration in color, the reader is referred to the web version of this article at www.liebertpub.com/ars

SCs, as previously reported (3, 15). On the other hand, APCs are defined by abundant PDGFRβ expression, which is thought to regulate pericyte and MSC migration and proliferation (5, 15). Interestingly, under unstimulated conditions, H_2O_2 increased APC migration, but not HUVEC or SVECs motility. Furthermore, oxidative stress completely inhibited the pro-migratory effect of VEGF on HUVECs, while leaving unmodified the PDGF-induced APC migration (Fig. 6A–F). No significant variation among the different conditions was observed with regard to the migratory activity of microvascular pericytes (Supplementary Fig. S5B).

A previous investigation indicates that Src Kinase acts as a sensor of ROS, activating different signaling pathways instrumental to redox-dependent promotion of cell migration and vascular remodeling (1, 31). Hence, we next asked whether Src is implicated in ROS-induced APC migration. To this end, the scratch assay was repeated in the presence of the Src inhibitor SU6656. Pretreatment of cells with SU6656 completely prevented the promotion of APC migration by H_2O_2, without affecting untreated cells (Fig. 6E, F).

Our previous work showed that APCs support EC network formation *in vitro* and neovascularization in models of peripheral and cardiac ischemia (5, 19). Therefore, here, we investigated the consequences of oxidative stress on APC-induced promotion of angiogenesis. We confirmed that APCs stimulate HUVEC and SVEC network formation capacity, with this effect remaining unaltered after APC preconditioning with H_2O_2 (Fig. 7A–D). This feature was further validated using a three-dimensional *in vitro* model of angiogenesis consisting of a spheroidal coculture system of APCs and HUVECs (21). After formation on a methylcellulose matrix, spheroids were embedded in a collagen gel, and the cumulative length of outgrowing capillary-like sprouts was quantified 12 h later. Spheroids made of ECs displayed a low baseline sprouting activity, whereas this feature was highly increased in the HUVEC/APC spheroids. Once again, H_2O_2 preconditioning did not impair APC capacity to improve endothelial sprouting activity (Supplementary Fig. S6A, B).

SOD3 silencing impairs APC-induced reparative vascularization in a mouse model of limb ischemia

We have previously shown that transplantation of APCs improves reparative angiogenesis in mouse models of peripheral and myocardial ischemia (5, 18, 19). In this work, we confirm that mice transplanted with naive APCs have an improved limb blood flow recovery from ischemia compared with mice given vehicle. In contrast, the administration of SOD3-silenced APCs failed to show any benefit on blood flow recovery of the ischemic muscle (Fig. 8A). Likewise, naïve APCs improved capillarization of the ischemic muscle, with this effect being negated by SOD3 silencing (Fig. 8B, C). These data suggest that SOD3 release by APCs could participate in the paracrine stimulation of vascular healing in the setting of ischemia.

Discussion

For a long time, pericytes have been considered passive elements filling the gaps between neighboring ECs. They gained attention with observations that diseases, such as diabetes and ischemia, can disrupt pericyte-EC interaction, leading to plasma extravasation, edema, and tissue damage. Furthermore, pericytes are therapeutically appealing because of their ability to differentiate into myocytes, satellite cells, and cardiomyocytes. We discovered the presence of clonogenic PCs that express typical pericyte markers in the adventitia of human veins (5). In models of ischemia, APCs transplantation promotes vascular growth and stabilization, through release of angiogenic factors and microRNAs and attraction of VEGF-expressing monocytes. Furthermore, APCs cooperate with resident SCs in the induction of cardiac repair (5, 18, 19). Hence, this newly identified PC population is endowed with pleiotropic functions that deserve mechanistic investigation.

In the present study, we have interrogated the APCs ability to cope with adverse oxidative conditions created by the exposure to H_2O_2. According to our standard operative protocol, the expansion of APCs from a small piece of human vein leads to the generation of 30–50 million viable cells at passage 7 in $\sim$10 weeks. Here, we confirm that repeatedly passaged APCs retain their original antigenic phenotype. Furthermore, we show for the first time that APCs, expanded to achieve quantities compatible with requirements of cell therapy in humans, are resistant to oxidative stress-induced apoptosis as compared with HUVECs and SVECs. The latter were obtained from the same source of APCs, thereby pinpointing properties intrinsic to the cell type rather than conferred by the particular local environment. In line, the unique resistance of APCs to oxidative stress was associated to high expression of a spectrum of antioxidant factors, which represent the major cellular defence against ROS. In particular, APCs express catalase, which may account for the protection from H_2O_2, and various SOD isoforms. A comparison of APCs and microvascular pericytes indicates a differential expression of SOD1 and SOD2, while the levels of catalase and SOD3 did not differ between the two cell populations. The latter antioxidant enzymes might suffice to confer similar resistance to ROS-induced cell damage, as documented when assessing the effect of H_2O_2 on apoptosis. In APCs, the functional relevance of this enzyme antioxidant machinery is also testified by a decreased tendency to accumulate protein carbonyl groups after hydrogen peroxide exposure as compared with ECs. Furthermore, after exposure to exogenous ROS, APCs show lower levels of pospho-γH2AX, a marker of DNA double-strand breaks, compared with ECs. These results suggest that ROS scavenging by antioxidant enzymes in APCs prevents protein or DNA damage.

Three SOD isoforms have been identified: the cytoplasmic SOD1, mitochondrial SOD2, and extracellular SOD3. In vascular tissue, SOD3 represents the principal SOD isoform. After secretion, SOD3 is anchored to the extracellular matrix and EC surface through binding to the heparan sulfate proteoglycan and fibulin-5. Owing to its location, the SOD3 plays an important role in modulating the levels of superoxide in the microvascular environment (13). Furthermore, SOD3 overexpression reportedly decreases ischemic tissue injury in animal models (20, 22). We found that APCs produce and secrete large amounts of SOD3, which might account for the reduction of oxidative stress-induced damage in neighboring cells, such as ECs. Although regarded as a pro-angiogenic factor for ECs through H_2O_2-induced activation of VEGF signaling (29), SOD3 also acts as a safeguard factor against potentially harmful ROS, especially—as observed in APCs—when combined with high catalase expression, enabling inactivation of SOD3-generated H_2O_2. The coordinated

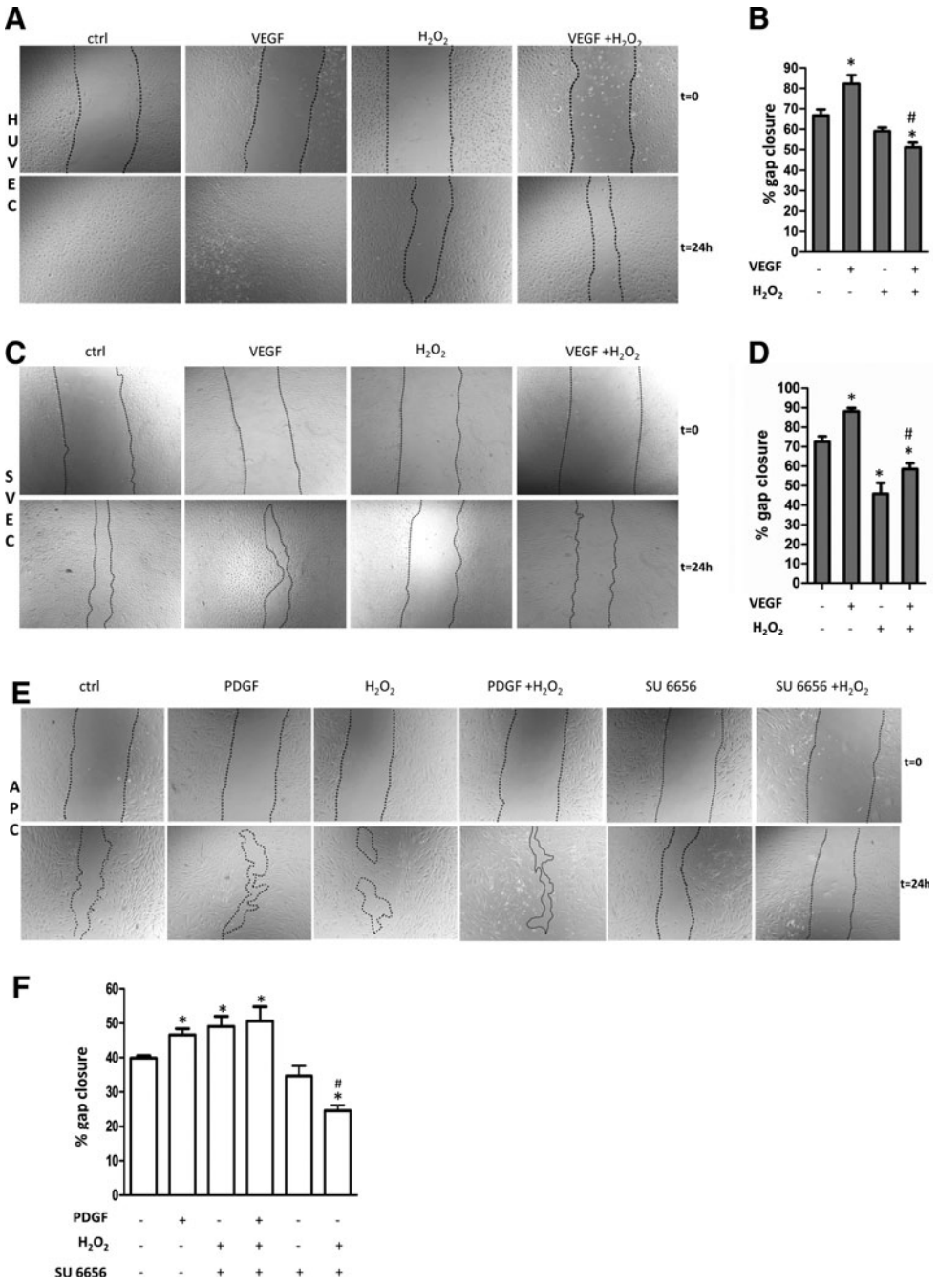

FIG. 6. Hydrogen peroxide inhibits HUVEC migration, whereas it increases APC migratory activity. (A) HUVEC monolayers were scratched and stimulated with vascular endothelial growth factor (VEGF) (100 ng/ml) in the presence or absence of H_2O_2 (250 μM). Phase-contrast images were collected after 24 h. H_2O_2 delayed HUVEC migration under basal conditions or VEGF stimulation. **(B)** Histograms indicating the percentage of gap closure: Values are means ± SEM of three independent experiments, $^*p < 0.05$ *versus* untreated cells; $^{\#}p < 0.005$ *versus* VEGF-treated cells. **(C)** SVEC monolayers were scratched and subjected to the same stimuli of HUVEC. **(D)** Histograms indicating the percentage of gap closure: Values are means ± SEM of three independent experiments, $^*p < 0.05$ *versus* untreated cells; $^{\#}p < 0.005$ *versus* VEGF-treated cells. **(E)** APC monolayers were scratched and incubated with PDGF (100 ng/ml) or SU6656 (5 μM) in the presence or absence of H_2O_2 (250 μM). H_2O_2 increased the unstimulated APC migration while leaving unmodified the pro-migratory effect of PDGF. Src inhibition by SU6656 inhibits the H_2O_2-induced migration of APCs, without affecting untreated cells. **(F)** Histograms illustrating the percentage of gap closure: Values are means ± SEM of three independent experiments, $^*p < 0.05$ *versus* untreated cells. $^{\#}p < 0.005$ *versus* H_2O_2 treated cells.

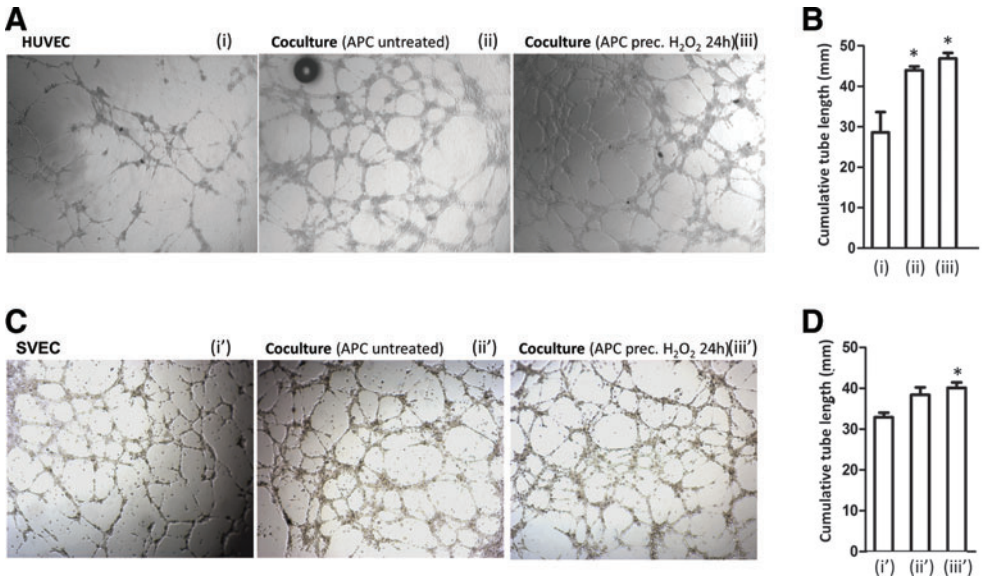

FIG. 7. Oxidative stress does not impair APC-induced support of network formation by endothelial cells. (A–D) Representative images (**A, C**) and bar graphs (**B, D**) showing the network formation by HUVECs and SVECs alone (**i, i'**) or HUVECs and SVECs in coculture with APCs (**ii, ii'**). Network formation was strongly enhanced in coculture compared with HUVECs alone. APC preconditioning with H_2O_2 (250 μM, 24 h) did not impair the enhancement of network formation by APCs (**iii, iii'**). Values are expressed as cumulative tube length per field and means ± SEM of three experiments performed in triplicate; $*p < 0.05$ *versus* HUVECs or SVECs alone. To see this illustration in color, the reader is referred to the web version of this article at www.liebertpub.com/ars

expression of SOD3 and catalase set up the conditions for an appropriate ''redox window,'' thereby preventing the detrimental effects of excessive or insufficient levels of ROS on SC/PC function. Importantly, we showed that the resistance toward oxidative stress is intrinsically associated to the stemness status of APCs, as differentiation into adipocytes led to a remarkable down-regulation of antioxidant genes.

The substantial increase in the toxic threshold of APCs enables these cells to maintain an intact migratory and pro-angiogenic activity after exposure to ROS levels that are

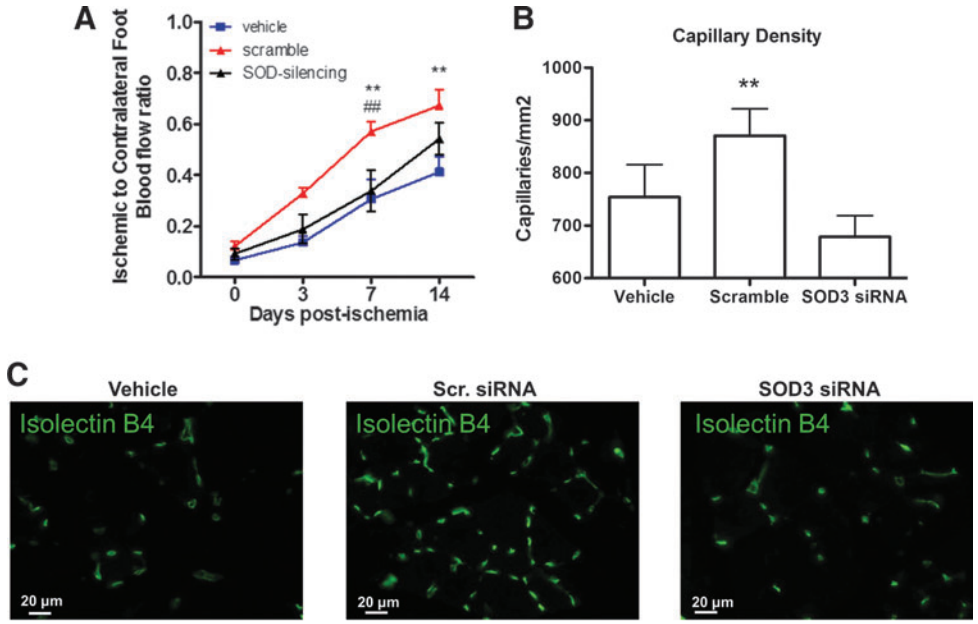

FIG. 8. SOD3 silencing impairs APC-induced reparative vascularization in a mouse model of limb ischemia. (A) Line graphs showing blood flow recovery from unilateral limb ischemia in mice given vehicle, scramble-transfected APCs, or SOD3-silenced APCs. Control (scramble-transfected) APCs improve blood flow recovery compared with vehicle or SOD3-silenced APCs ($n = 9$ animals per group). **(B, C)** Representative pictures and bar graphs show increased capillary density in muscles injected with scramble-transfected APCs compared with vehicle or SOD3-silenced APCs at 14 days after ischemia. Values are mean ± SEM ($n = 7$ animals per group), $**p < 0.01$ SOD3 *versus* scramble group; $^{\#\#}p < 0.01$ *versus* Vehicle. To see this illustration in color, the reader is referred to the web version of this article at www.liebertpub.com/ars

detrimental for other vascular cells. Importantly, APC proliferation was increased after exposure to H_2O_2 levels below the threshold at which toxicity becomes apparent. This result is in line with our previous observation that APCs thrive in the harsh environment of an ischemic tissue. Src kinase is the main sensor of intracellular redox state, and its activation is thought to play an important role in oxidative stress-induced cell migration and vascular remodeling. The inhibition of Src kinase blunted the pro-migratory effect of H_2O_2 on APCs, thus confirming that Src kinase is instrumental to oxidative stress-dependent migration of APCs. Nonetheless, redox homeostasis is finely regulated in mesenchymal cells. An intertwinement of Src kinase with other main factors should be taken into consideration. For instance, Src kinase takes part in Nuclear factor (erythroid-derived 2)-like 2 (Nrf-2) regulation. Nrf-2 is one of the primary defense mechanisms against pro-oxidant stimuli. When activated, Nrf-2 translocates to the nucleus, where it binds to the antioxidant response elements of cytoprotective genes, such as SODs, leading to up-regulation of their expression. This early response is followed by a late phase that leads to Src kinase-mediated degradation of Nrf2, resulting in a negative feedback (26). We cannot exclude the activation of Nrf-2 by H_2O_2 and later involvement of Src into the switching off of Nrf-2 cycle, as we did not observe any variation of the Nrf-2 target genes after 24 h exposure to H_2O_2 (data not shown). Furthermore, to what extent Nrf-2 controls either the basal or inducible expression of its effector genes is not yet clear.

Finally, we have investigated the consequences of SOD3 silencing on APC biological activities both *in vitro* and *in vivo*. Interestingly, SOD3 silencing was not sufficient to abrogate the SVP resistance to oxidative stress. This result was somehow expected, because redundant antioxidant mechanisms participate in the maintenance of the redox balance. Accordingly, global inhibition of SODs enhanced the increase in ROS levels caused by H_2O_2, a result that was associated with manifestation of APC apoptosis. Since SOD3 is secreted into the extracellular space, this isoform might take part in the paracrine cross-talk between APCs and neighboring cells. This represents a key of interpretation for the apparent discrepancy between the lack of effect of SOD3 silencing on APC viability and the interference of SOD3 silencing on reparative angiogenesis in *in vivo* studies. A recent study using SOD3 gene therapy in rats with limb ischemia showed a reduction in cell apoptosis compared with control animals, which was ascribed to the activation of pro-proliferative and anti-apoptotic Erk1/2 and Akt pathways, associated inhibition of forkhead box protein-O3a, and inhibition of oxidative mechanisms (22). Together, these data highlight the complexity of SOD3-derived effects on tissue injury recovery.

Materials and Methods

Ethics

Studies complied with the principles stated in the ''*Declaration of Helsinki*.'' Patients gave written informed consent to participate. APCs and SVECs were obtained from CABG patients at the University of Bristol, under ethical approval 06/Q2001/197. Microvascular pericytes were obtained from muscular biopsies in patients referring to MultiMedica IRCCS for saphenectomy, under ethical approval 11/2009.

Cell culture

APCs and SVECs were isolated from vein leftovers, as previously described (5). HUVECs were purchased from Lonza. All cell populations were cultured on fibronectin (10 μg/ml)/gelatin (0.01%) in endothelial growth medium containing 2% FBS (Lonza) and used at passage 7. To induce oxidative stress, cells were exposed to increasing concentrations of H_2O_2 (1–250 μM).

Microvascular pericytes were isolated through enzymatic digestion of muscle biopsies using collagenase type II (9). Isolated cells were cultured on plastic for 2 weeks in αMEM medium plus 20% fetal bovine serum until colonies formed. Expanded cells stained positive for pericyte markers such as NG2 and CD146 and in culture acquired the skeletal muscle marker CD56, as demonstrated by flow cytometry and immunofluorescent staining procedures. Microvascular pericytes were used at passage 7.

APC differentiation

Differentiation of APCs into adipocytes was induced by plating cells at a high density (2×10^4/cm^2) in DMEM-high glucose supplemented with 5% horse serum, 10^{-6} M dexamethasone, 0.2 mM indomethacin, 0.01 mg/ml insulin, and 0.05 mM 3.isobutyl.l.methyl-xanthine (all from Sigma-Aldrich Corp). Differentiation was assessed by Oil Red O staining (Sigma).

Flow cytometry analysis

APCs were stained for surface antigen expression using combinations of the following antibodies: anti-CD90, anti-CD-105, anti-CD31, anti-CD44, and anti-CD45 (all from BD Biosciences). An aliquot of cells was stained with secondary antibody only as an internal control of specificity. For each test, 2×10^5 to 1×10^6 total events were acquired on an FACS Canto II flow cytometer (BD). FACS Diva software (BD) was used for acquisition and data analysis.

Immunocytochemistry

For immunofluorescence microscopy, cells were fixed in 4% buffered paraformaldehyde and permeabilized (in case of detection of intra-cytoplasmatic antigens) with 0.1% TritonX before incubation with primary antibody for the platelet-derived growth factor receptor β (PDGFRβ, 1:50; Cell signaling), Vimentin (1:20; Abcam), NG2 (1:150; Millipore), Desmin (1:20; Chemicon), α-smooth muscle actin (1:50; Dako), α-sarcomeric actin (α-SMA, 1:200; Sigma), and CD31 (1:50; Dako) VE-Cadherin (1:50; Santa Cruz Biotechnology). AlexaFluor-labeled secondary antibodies (Molecular Probes/Invitrogen) were employed to detect primary antibodies. Staining with 4',6-diamidino-2-phenylindole (DAPI; Vector Laboratories, Inc.) was used to identify nuclei. Immunocytochemistry was performed by utilizing the peroxidase-conjugated EnVision system (Dako).

Functional assays

After seeding in a 96- or 48-well of a fibronectin/gelatin-coated plate, APCs ($\sim$6000/cm^2) or ECs ($\sim$16,000/cm^2) were allowed to settle for 24 h (37°C, 5% CO_2). Then, cells were incubated for 30 min in the absence or presence of various inhibitors before H_2O_2 treatment.

Confocal microscopy analysis of ROS. Mitochondrial imaging of live cells was performed in 96-well glass bottom plates (Matrical Bioscience) using a confocal microscope (Leica SP5; Milton Keynes) with a 40× water immersion objective. For ROS detection, cells were loaded with Mitotracker red CM-H_2XRos (0.1 μM, 30 min; Invitrogen) and rinsed with EBM-2 media. Fluorescence intensity was measured using a 561 nm laser for excitation and greater than 580 nm for emission and quantified using Volocity program (Improvision).

Apoptosis assay. Apoptosis was assessed by a Caspase Assay (Promega-Glo® 3/7 Assay) following the manufacturer's instructions. Briefly, after H_2O_2 treatment, the medium was removed and replaced with fresh medium. Then, the Caspase-Glo substrate with buffer mix was added to each well, and plates were incubated away from light on a shaker for 30 min at room temperature. In some experiments, cells were preincubated for 30 min with the SOD inhibitor DDC (10 μM; SIGMA), before H_2O_2 treatment at the indicated doses for 24 h. Absorbance was recorded at 485 nm using a 96-well plate reader (Promega). Each experiment was performed in triplicate and repeated thrice.

Proliferation assay. To study the effect of ROS on cell proliferation, BrdU (10 μM) was added to the medium just before cell exposure to H_2O_2. BrdU incorporation was measured with an immunofluorescence assay kit (Roche) following the manufacturer's instructions. Briefly, APCs were fixed and made permeable with FixDenat solution for 20 min, then incubated with monoclonal anti-BrdU peroxidase-conjugated antibody (anti-BrdU-POD) for 90 min. Bound anti-BrdU-POD was detected by a substrate reaction, and absorbance was recorded at 450 nm using a 96-well plate ELISA reader. Six wells per condition were plated in three independent experiments.

Migration assay. After reaching confluence, the cell monolayer was scratched using a P1000 tip at the centre of the well. Then, the medium was exchanged to complete EGM with 2 mM of Hydroxyurea (Sigma) to induce growth arrest. To investigate the mechanism responsible for inhibition of cell migration by oxidative stress, the assay was performed in the presence of the Src inhibitor SU6656 (5 μM; Calbiochem) or vehicle, which were added 30 min before cell exposure to H_2O_2. Images were taken using a bright-field inverted microscope (at 5×). The percentage of gap closure was calculated using the Zeiss Axiovert software (Carl Zeiss Microscopy), measuring five distances per field of view of the leading edges at the time of the scratch and 24 h later. The calculation is as follows: %gap = 100 − (100* D24/D0). Each experiment was performed in triplicate and repeated thrice.

In vitro matrigel assay. To assess the effect of ROS on the APC ability to promote EC network formation, untreated or H_2O_2-preconditioned APCs were mixed with HUVECs (1:4 ratio of APCs to HUVECs, respectively) and seeded in 96-well plates, previously filled with 40 μl of complete Matrigel (BD Bioscience) and placed at 37°C for 20 min to enable matrix solidification. For each condition, triplicate wells were set up and experiments were repeated in three independent experiments. HUVECs alone served as a normalization control. The cells were carefully dispensed onto the solidified Matrigel and allowed to settle and form networks for 18 h, after which pictures were taken using a bright-field inverted microscope. The length of networks was calculated using the Image-Pro Plus software (Media Cybernetics) on images taken at 40× magnification.

Spheroid generation and sprouting assay. Coculture spheroids were generated as previously described(21). In brief, ~750 HUVECs and ~190 APCs (ratio 4 ÷ 1) were suspended in EGM-2 containing 0.25% (w/v) methylcellulose (Sigma) and seeded in round-bottom 96-well plates (150 μl/well). Spheroids were cultured under these conditions for at least 24 h. For sprouting assay, spheroids were collected after 24 h and embedded into collagen gels mixed with 0.5 ml of EGM-2 containing 40% FBS and 0.5% (w/v) methylcellulose at room temperature. Then, ~50 spheroids were added to the solution. The spheroid-containing gel was rapidly transferred into prewarmed 24-well plates (400 μl/well) and allowed to polymerize 2–3 min, after which 0.1 ml EGM-2 was pipetted on the top of the gel. Pictures of the sprouting were taken after 6 and 12 h. The sprouting capacity of HUVECs alone was used as a control. *In vitro* angiogenesis was digitally quantified by measuring the length of the sprouts that had grown out of each spheroid using the Zeiss' Axiovert software.

γH2AX staining. Immunofluorescent staining for phospho-histone H2A.X (Ser139) was used to detect DNA damage in HUVECs and APCs after treatment with H_2O_2 for 24 h. Briefly, cells were fixed in 4% PFA, permeabilized for 10 min in PBS/0.1% Triton X-100, and blocked with 10% goat serum for 30 min at RT. After incubation with mouse anti-phospho-histone H2A.X (Ser139) antibody, clone JBW301 (Millipore) for 2 h at 37°C in a dark humidified chamber, Alexa 488-conjugated goat anti-mouse secondary antibody (Invitrogen) was applied. DAPI was used to detect nuclei. Cells with only secondary antibody staining were used as negative controls. The number of positive nuclei on the total number of nuclei was assessed.

Protein carbonyl determination. Protein carbonyls were determined using the Protein Carbonyl ELISA kit (Enzo Life Sciences) according to the manufacturer's instructions. Twenty μg of protein from each sample were derivatized with dinitrophenylhyidrazine (DNPH). Derivatized proteins were then adsorbed to an ELISA plate and probed with biotinylated anti-DNP antibody followed by streptavidin-linked horseradish peroxidase. The absorbance was read at 450 nm using a spectrophotometer plate reader. Cell lysates were assayed in duplicate, and protein carbonyl quantification was normalized using the control samples.

Gene arrays

One hundred nanogram of each RNA sample was labeled and hybridized onto Agilent Whole Human Genome 4x44K microarrays according to the Agilent One-Color Microarray-Based Gene Expression Analysis Protocol. Arrays were scanned on an Agilent Microarray Scanner, and raw data analysis was performed using the Feature Extraction 10.5.1 software (Agilent). For statistical analysis of microarray

experiments, all data analysis and all data preprocessing were performed in R/Bioconductor (14, 34). Data preprocessing included the following steps: background correction using Agilent spatial detrending background estimate, averaging of replicate spots, log2-transformation, k-nearest-neighbor imputation of missing values, unsupervised filtering (IQR threshold) to get rid of uninformative probes (low variance), and quantile normalization. For inference statistics, the linear modeling functions provided by the Limma package were used. Results of gene arrays have been uploaded on www.ncbi.nlm.nih.gov/geo/with reference GSE50758

SOD3 knockdown

APCs were transfected with SOD3 siRNA (50 n*M*) or scramble sequence (50 n*M*), both from Qiagen) for 72 h using commercially available transfection lipofectamine agent RNAiMAX (Invitrogen). After 72 h, APCs were trypsinized and transplanted into mouse limb muscle (80×10^3 cells/animal). Effective SOD3 silencing was tested *in vitro* by RT-PCR and western blotting.

RNA isolation and quantitative RT-PCR

Total RNA was extracted from APCs, HUVECs, or SVECs using Trizol (Invitrogen) according to the manufacturer's instructions. One microgram of total RNA was reverse transcribed using Qiagen reverse-transcriptase kit, followed by amplification of cDNA using QuantiTect primers for SOD, catalase, and internal control 18S (all from Qiagen).

Protein extraction and Western blotting

Proteins were extracted from APCs, HUVECs, or SVECs using a commercial kit (Roche). Protein concentration was determined using the Bio-Rad protein assay reagent (Bio-Rad). Detection of proteins by western blot analysis was done following separation of an equal amount of cell extracts on SDS-polyacrylamide gels. Proteins were transferred to polyvinylidene difluoride membranes (PVDF; Amersham-Pharmacia) and probed with the following antibodies: SOD1 (0.1 μg/ml; R&D System), SOD2 (1:1000; GeneTex), SOD3 (0.1 μg/ml; R&D System), and Catalase (1:1000; Calbiochem). Tubulin (Cell Signaling; 1:1000) was used as a loading control. For detection, secondary antibody goat anti-rabbit or anti-mouse or donkey anti-goat conjugated to horseradish peroxidase (all from Santacruz; 1:5000) were used, followed by chemiluminescence reaction (ECL; Amersham Pharmacia). Density of the bands was analyzed using Image-J (NIH) software, and data were expressed as fold changes.

Conditioned media preparation

To obtain CCM, cells were grown to 70% confluence and incubated with fresh medium, without the addition of FBS, for 48 h. Then CCM was collected and concentrated (50×, Amicon ultra; Millipore).

In vivo *studies*

Experiments were performed in accordance with the *Guide for the Care and Use of Laboratory Animals* (Institute of Laboratory Animal Resources, 1996) and with approval of the British Home Office and the University of Bristol. Male 12-week-old CD1 mice (Harlan) underwent unilateral limb ischemia as previously described (5). At the occasion of ischemia induction, 8×10^4 scramble or SOD3-silenced APCs (passage 7) or vehicle (DMEM, 30 μl) were injected into three different points of the ischemic adductor muscle ($n = 9$ mice per group). Blood flow recovery was followed up for 14 days by laser Doppler flowmetry as previously reported (5). Sections (3 μm) from paraffin-embedded adductor muscles were stained with isolectin B4 to recognize ECs and calculate capillary density.

Statistical analysis

Values are presented as mean ± SEM. Analyses were performed with GraphPad Prism 6 (GraphPad Software). A comparison between groups was performed using one-way ANOVA. Furthermore, two-way ANOVA was used when evaluating the effect of different doses of H_2O_2 on APCs as compared with ECs in functional assays. Mann–Whitney test for nonparametric data was used to plot histology data. Linear regression analysis was performed between log values of gene expression and therapeutic outcomes. Probability values (p) less than 0.05 were considered significant.

Acknowledgments

The authors thank Alan Leard for his technical and helpful support and Helen Spencer for valuable advice and revision. This study was supported by the British Heart Foundation (project grant ''Human pericyte progenitor cells and cardiac progenitor cells for specialized stimulation of neovascularization and cardiomyogenesis of the infarcted heart,'' the Medical Research Council (project grant ''Manufacture scale up of human pericyte progenitor cells for regenerative medicine'') and the NIHR Bristol Cardiovascular Biomedical Research Unit.

Author Disclosure Statement

No competing financial interests exist.

References

1. Abe J, Takahashi M, Ishida M, Lee JD, and Berk BC. c-Src is required for oxidative stress-mediated activation of big mitogen-activated protein kinase 1. *J Biol Chem* 272: 20389–20394, 1997.
2. Anilkumar N, San Jose G, Sawyer I, Santos CX, Sand C, Brewer AC, Warren D, and Shah AM. A 28-kDa splice variant of NADPH oxidase-4 is nuclear-localized and involved in redox signaling in vascular cells. *Arterioscler Thromb Vasc Biol* 33: e104–e112, 2013.
3. Ball SG, Shuttleworth CA, and Kielty CM. Vascular endothelial growth factor can signal through platelet-derived growth factor receptors. *J Cell Biol* 177: 489–500, 2007.
4. Bouacida A, Rosset P, Trichet V, Guilloton F, Espagnolle N, Cordonier T, Heymann D, Layrolle P, Sensebe L, and Deschaseaux F. Pericyte-like progenitors show high immaturity and engraftment potential as compared with mesenchymal stem cells. *PLoS One* 7: e48648, 2012.
5. Campagnolo P, Cesselli D, Al Haj Zen A, Beltrami AP, Krankel N, Katare R, Angelini G, Emanueli C, and Madeddu P. Human adult vena saphena contains perivascular

progenitor cells endowed with clonogenic and proangiogenic potential. *Circulation* 121: 1735–1745, 2010.
6. Cocco D, Calabrese L, Rigo A, Argese E, and Rotilio G. Re-examination of the reaction of diethyldithiocarbamate with the copper of superoxide dismutase. *J Biol Chem* 256: 8983–8986, 1981.
7. Crisan M, Yap S, Casteilla L, Chen CW, Corselli M, Park TS, Andriolo G, Sun B, Zheng B, Zhang L, Norotte C, Teng PN, Traas J, Schugar R, Deasy BM, Badylak S, Buhring HJ, Giacobino JP, Lazzari L, Huard J, and Peault B. A perivascular origin for mesenchymal stem cells in multiple human organs. *Cell Stem Cell* 3: 301–313, 2008.
8. Dalle-Donne I, Rossi R, Giustarini D, Milzani A, and Colombo R. Protein carbonyl groups as biomarkers of oxidative stress. *Clin Chim Acta* 329: 23–38, 2003.
9. Dellavalle A, Maroli G, Covarello D, Azzoni E, Innocenzi A, Perani L, Antonini S, Sambasivan R, Brunelli S, Tajbakhsh S, and Cossu G. Pericytes resident in postnatal skeletal muscle differentiate into muscle fibres and generate satellite cells. *Nat Commun* 2: 499, 2011.
10. Dernbach E, Urbich C, Brandes RP, Hofmann WK, Zeiher AM, and Dimmeler S. Antioxidative stress-associated genes in circulating progenitor cells: evidence for enhanced resistance against oxidative stress. *Blood* 104: 3591–3597, 2004.
11. Eirew P, Kannan N, Knapp DJ, Vaillant F, Emerman JT, Lindeman GJ, Visvader JE, and Eaves CJ. Aldehyde dehydrogenase activity is a biomarker of primitive normal human mammary luminal cells. *Stem Cells* 30: 344–348, 2012.
12. Fleissner F and Thum T. Critical role of the nitric oxide/reactive oxygen species balance in endothelial progenitor dysfunction. *Antioxid Redox Signal* 15: 933–948, 2011.
13. Fukai T and Ushio-Fukai M. Superoxide dismutases: role in redox signaling, vascular function, and diseases. *Antioxid Redox Signal* 15: 1583–1606, 2011.
14. Gentleman R. *Bioinformatics and computational biology solutions using R and Bioconductor*. New York: Springer Science+Business Media, 2005, pp. xix, 473.
15. Gomes SA, Rangel EB, Premer C, Dulce RA, Cao Y, Florea V, Balkan W, Rodrigues CO, Schally AV, and Hare JM. S-nitrosoglutathione reductase (GSNOR) enhances vasculogenesis by mesenchymal stem cells. *Proc Natl Acad Sci U S A* 110: 2834–2839, 2013.
16. Ingram DA, Mead LE, Moore DB, Woodard W, Fenoglio A, and Yoder MC. Vessel wall-derived endothelial cells rapidly proliferate because they contain a complete hierarchy of endothelial progenitor cells. *Blood* 105: 2783–2786, 2005.
17. Jang YY and Sharkis SJ. A low level of reactive oxygen species selects for primitive hematopoietic stem cells that may reside in the low-oxygenic niche. *Blood* 110: 3056–3063, 2007.
18. Katare R, Riu F, Mitchell K, Gubernator M, Campagnolo P, Cui Y, Fortunato O, Avolio E, Cesselli D, Beltrami AP, Angelini G, Emanueli C, and Madeddu P. Transplantation of human pericyte progenitor cells improves the repair of infarcted heart through activation of an angiogenic program involving micro-RNA-132. *Circ Res* 109: 894–906, 2011.
19. Katare RG and Madeddu P. Pericytes from human veins for treatment of myocardial ischemia. *Trends Cardiovasc Med* 23: 66–70, 2013.
20. Kim HW, Lin A, Guldberg RE, Ushio-Fukai M, and Fukai T. Essential role of extracellular SOD in reparative neovascularization induced by hindlimb ischemia. *Circ Res* 101: 409–419, 2007.
21. Korff T, Kimmina S, Martiny-Baron G, and Augustin HG. Blood vessel maturation in a 3-dimensional spheroidal coculture model: direct contact with smooth muscle cells regulates endothelial cell quiescence and abrogates VEGF responsiveness. *FASEB J* 15: 447–457, 2001.
22. Laatikainen LE, Incoronato M, Castellone MD, Laurila JP, Santoro M, and Laukkanen MO. SOD3 decreases ischemic injury derived apoptosis through phosphorylation of Erk1/2, Akt, and FoxO3a. *PLoS One* 6: e24456, 2011.
23. Majesky MW, Dong XR, Hoglund V, Daum G, and Mahoney WM, Jr. The adventitia: a progenitor cell niche for the vessel wall. *Cells Tissues Organs* 195: 73–81, 2012.
24. Mangialardi G, Katare R, Oikawa A, Meloni M, Reni C, Emanueli C, and Madeddu P. Diabetes causes bone marrow endothelial barrier dysfunction by activation of the RhoA-Rho-associated kinase signaling pathway. *Arterioscler Thromb Vasc Biol* 33: 555–564, 2013.
25. Moreb JS. Aldehyde dehydrogenase as a marker for stem cells. *Curr Stem Cell Res Ther* 3: 237–246, 2008.
26. Niture SK, Jain AK, Shelton PM, and Jaiswal AK. Src subfamily kinases regulate nuclear export and degradation of transcription factor Nrf2 to switch off Nrf2-mediated antioxidant activation of cytoprotective gene expression. *J Biol Chem* 286: 28821–28832, 2011.
27. Ogasawara MA and Zhang H. Redox regulation and its emerging roles in stem cells and stem-like cancer cells. *Antioxid Redox Signal* 11: 1107–1122, 2009.
28. Oikawa A, Siragusa M, Quaini F, Mangialardi G, Katare RG, Caporali A, van Buul JD, van Alphen FP, Graiani G, Spinetti G, Kraenkel N, Prezioso L, Emanueli C, and Madeddu P. Diabetes mellitus induces bone marrow microangiopathy. *Arterioscler Thromb Vasc Biol* 30: 498–508, 2010.
29. Oshikawa J, Urao N, Kim HW, Kaplan N, Razvi M, McKinney R, Poole LB, Fukai T, and Ushio-Fukai M. Extracellular SOD-derived H2O2 promotes VEGF signaling in caveolae/lipid rafts and post-ischemic angiogenesis in mice. *PLoS One* 5: e10189, 2010.
30. Peault B. Are mural cells guardians of stemness?: From pluri- to multipotency via vascular pericytes. *Circulation* 125: 12–13, 2012.
31. Saito A, Hayashi T, Okuno S, Nishi T, and Chan PH. Oxidative stress affects the integrin-linked kinase signaling pathway after transient focal cerebral ischemia. *Stroke* 35: 2560–2565, 2004.
32. Siwik DA, Tzortzis JD, Pimental DR, Chang DL, Pagano PJ, Singh K, Sawyer DB, and Colucci WS. Inhibition of copper-zinc superoxide dismutase induces cell growth, hypertrophic phenotype, and apoptosis in neonatal rat cardiac myocytes *in vitro*. *Circ Res* 85: 147–153, 1999.
33. Spinetti G, Cordella D, Fortunato O, Sangalli E, Losa S, Gotti A, Carnelli F, Rosa F, Riboldi S, Sessa F, Avolio E, Beltrami AP, Emanueli C, and Madeddu P. Global remodeling of the vascular stem cell niche in bone marrow of diabetic patients: implication of the microRNA-155/FOXO3a signaling pathway. *Circ Res* 112: 510–522, 2013.
34. Team RC. *R: A Language and Environment for Statistical Computing*. Vienna, Austria: R Foundation for Statistical Computing, 2012. www.lsw.uni-heidelberg.de/users/christlieb/teaching/UKStaSS10/R-refman.pd
35. Torsney E and Xu Q. Resident vascular progenitor cells. *J Mol Cell Cardiol* 50: 304–311, 2011.

36. Urao N, Inomata H, Razvi M, Kim HW, Wary K, McKinney R, Fukai T, and Ushio-Fukai M. Role of nox2-based NADPH oxidase in bone marrow and progenitor cell function involved in neovascularization induced by hindlimb ischemia. *Circ Res* 103: 212–220, 2008.
37. Urao N, McKinney RD, Fukai T, and Ushio-Fukai M. NADPH oxidase 2 regulates bone marrow microenvironment following hindlimb ischemia: role in reparative mobilization of progenitor cells. *Stem Cells* 30: 923–934, 2012.
38. Warren LA and Rossi DJ. Stem cells and aging in the hematopoietic system. *Mech Ageing Dev* 130: 46–53, 2009.

Address correspondence to:
Prof. Paolo Madeddu
Expermental Cardiovascular Medicine
School of Clinical Sciences
University of Bristol
Bristol BS2 8HW
United Kingdom

E-mail: mdprm@bristol.ac.uk

Date of first submission to ARS Central, May 12, 2013; date of final revised submission, January 31, 2014; date of acceptance, February 8, 2014.

Abbreviations Used

α-SMA = α-smooth muscle actin
APC = adventitia-derived progenitor cell
CABG = coronary artery bypass graft
CCM = conditioned culture medium
CM = conditioned medium
DDC = diethyldithiocarbamate
EC = endothelial cell
EPC = endothelial progenitor cell
HUVEC = human umbilical vein endothelial cell
MPs = muscle pericytes
NAC = N-acetyl cysteine
PDGF = platelet derived growth factor
ROS = reactive oxygen species
SC = stem cell
SOD = superoxide dismutase
SVEC = saphenous vein-derived endothelial cell
VEGF = vascular endothelial growth factor